

Typicality Approach to the Optical Conductivity in Thermal and Many-Body Localized Phases

Robin Steinigeweg,^{1,*} Jacek Herbrych,^{2,3,†} Frank Pollmann,^{4,‡} and Wolfram Brenig^{5,§}

¹*Department of Physics, University of Osnabrück, D-49069 Osnabrück, Germany*

²*Department of Physics, University of Crete, GR-71003 Heraklion, Greece*

³*Cretan Center for Quantum Complexity and Nanotechnology, University of Crete, GR-71003 Heraklion, Greece*

⁴*Max-Planck-Institut für Physik komplexer Systeme, D-01187 Dresden, Germany*

⁵*Institute for Theoretical Physics, Technical University Braunschweig, D-38106 Braunschweig, Germany*

(Dated: June 21, 2016)

We study the frequency dependence of the optical conductivity $\text{Re}\sigma(\omega)$ of the Heisenberg spin-1/2 chain in the thermal and near the transition to the many-body localized phase induced by the strength of a random z -directed magnetic field. Using the method of dynamical quantum typicality, we calculate the real-time dynamics of the spin-current autocorrelation function and obtain the Fourier transform $\text{Re}\sigma(\omega)$ for system sizes much larger than accessible to standard exact-diagonalization approaches. We find that the low-frequency behavior of $\text{Re}\sigma(\omega)$ is well described by $\text{Re}\sigma(\omega) \approx \sigma_{\text{dc}} + a|\omega|^\alpha$, with $\alpha \approx 1$ in a wide range within the thermal phase and close to the transition. We particularly detail the decrease of σ_{dc} in the thermal phase as a function of increasing disorder for strong exchange anisotropies. We further find that the temperature dependence of σ_{dc} is consistent with the existence of a mobility edge.

PACS numbers: 05.60.Gg, 71.27.+a, 75.10.Jm

Introduction. Many-body localization (MBL) generalizes the concept of Anderson localization [1] to interacting systems. In a pioneering work [2], Basko, Aleiner, and Altshuler showed perturbatively that the Anderson insulator is stable to small interactions. Thus, an isolated quantum many-body system can undergo a dynamical phase transition from a thermal phase to an MBL phase where eigenstate thermalization [3–5] breaks down. Subsequent numerical works further revealed the richness of disordered many-body systems [6–9]. A characteristic property of MBL systems is a logarithmic growth of entanglement after a global quench [10, 11], which has led to a phenomenological understanding in terms of locally conserved quantities [12–14]. An exciting aspect of MBL is that it allows to protect quantum orders at finite energy densities (both symmetry breaking and topological ones), which would melt in thermal phases [15–19]. On the experimental side, first observations of MBL in optical-lattice systems have been made by studying quantum quenches in disordered systems of interacting particles [20]. Furthermore, the I - V characteristics of amorphous iridium-oxide reveal an insulating state where MBL might play a role [21].

In the ongoing discussion of MBL, a central model is the spin-1/2 XXZ chain with a spatially random z -directed magnetic field, being equivalent to interacting spinless fermions in a random on-site potential of strength W . Furthermore, the XXZ chain is a fundamental model for the study of transport and relaxation in low dimensions [22] and relevant to the physics of quasi one-dimensional quantum magnets [23–28], cold atoms in optical lattices [29], and nanostructures [30], as well as to physical questions in a much broader context [31, 32].

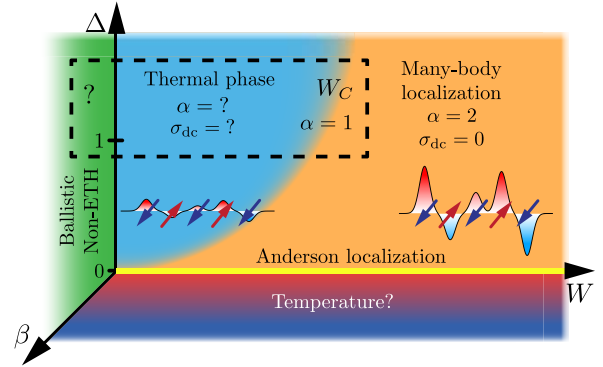


FIG. 1. (Color online) Dynamical phase diagram (sketch) of disordered spin-1/2 XXZ chains. Issues studied in this paper: Scaling of dc conductivity σ_{dc} and low-frequency exponent α for strong interactions $\Delta \geq 1$ and disorders $W \geq 0$ up to the MBL transition; temperature dependence and existence of mobility edge; typicality in finite systems with $W > 0$.

This model is also of paramount interest due to its remarkably rich dynamical phase diagram, manifest in the frequency- and temperature-dependent optical conductivity $\sigma(\omega, T)$. Despite integrability of the disorder-free XXZ chain, $W = 0$, the exact calculation of $\sigma(\omega, T)$ at $T \neq 0$ has been and continues to be a challenge to theory and is an important goal of new analytical and numerical techniques. While it has become clear that, for small particle-particle interactions $\Delta < 1$, $\sigma(\omega, T)$ features a non-dissipative Drude contribution at $\omega = 0$ and any $T \geq 0$ [33–45], much less is known on the dynamics at $\omega \neq 0$. Yet, signatures of diffusion, e.g., with a well-behaved limit $\omega \rightarrow 0$, have been found only for strong

$\Delta > 1$ and high T [46–48] as well as for $\Delta = 1$ and very low T [49–51].

Perturbations, such as spin-phonon coupling [52–54], dimerization [55, 56], interactions between further neighbors [57, 58] or different chains [24, 25, 59–64], break integrability of the XXZ chain and therefore add another layer of complexity. In this context, improving numerical approaches is imperative to progress in understanding. Within the class of relevant perturbations, disorder plays a remarkable role since it goes along with MBL as a new dynamical state of matter. Early on, a numerical work based on Lanczos diagonalization [65] found that, at $\Delta = 1$ and $W = 1$, the low- ω optical conductivity at high T follows the power law $\text{Re } \sigma(\omega) \approx \sigma_{\text{dc}} + a |\omega|^\alpha$, with $\alpha \approx 1$, being different from Mott’s law for the Anderson insulator $\alpha \approx 2$. Such α was also observed for small but finite Δ and in a wider range of W [66]. A more recent theoretical study [67] has suggested that $\alpha \rightarrow 1$ when approaching the MBL transition from the localized ($\sigma_{\text{dc}} = 0$) side, attributed to rare metallic regions, in contrast to $\alpha \approx 2$, due to rare resonant pairs deep in the localized phase.

In this paper, we study the optical conductivity in disordered systems using complementary numerical methods, with a particular focus on dynamical quantum typicality (DQT) [43, 44, 68] (see also [69–80]). This method employs the fact a single pure state can exhibit properties identical to that of the complete statistical ensemble. This fact has been demonstrated in nontrivial phases of the disorder-free XXZ chain and allows to study the long-time dynamics of quantum systems with Hilbert spaces being much larger than those accessible to standard ED approaches. While in localized phases it is clear that a single *eigenstate* cannot be a typical representative, i.e., the eigenstate thermalization hypothesis (ETH) [3–5] is not satisfied, we show for finite systems that DQT, which is *different* from ETH, works well, i.e., still the overwhelming majority of states drawn at random from a high-dimensional Hilbert space are typical.

To outline, we apply DQT to disordered XXZ chains and demonstrate that a single pure state can indeed represent the full statistical ensemble within the entire range from the thermal to the MBL phase. In particular, we find that $\text{Re } \sigma(\omega) \approx \sigma_{\text{dc}} + a |\omega|^\alpha$ with $\alpha \approx 1$ in a wide range of parameters within the thermal phase and close to the transition. Moreover, we detail the dependence of σ_{dc} on W and connect to known results on either very small or very large W . Finally, we determine the T dependence of σ_{dc} down to low T in the thermal phase. We find that this dependence is consistent with the existence of an MBL mobility edge. Thus, our results provide for a comprehensive picture of dynamical phases in disordered XXZ chains, as illustrated in Fig. 1.

Model. We study the antiferromagnetic XXZ spin-1/2 chain with periodic boundary conditions, given by ($\hbar =$

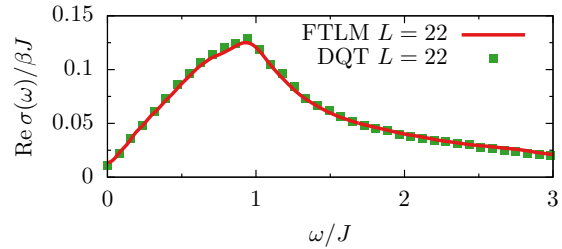


FIG. 2. (Color online) Comparison of DQT ($tJ \leq 40$) and FTLM ($M = 400$): $\text{Re } \sigma(\omega)$ at $\beta \rightarrow 0$, $\Delta = 1$, and $W/J = 2$ for $L = 22$ and $N = 200$. The excellent agreement clearly shows the validity of typicality. Such agreement is also found for other values of W , see [87].

1)

$$H = J \sum_{r=1}^L (S_r^x S_{r+1}^x + S_r^y S_{r+1}^y + \Delta S_r^z S_{r+1}^z + B_r S_r^z), \quad (1)$$

where $S_r^{x,y,z}$ are the components of spin-1/2 operators at site r . $J > 0$ is the exchange coupling constant, L the total number of sites, and Δ the anisotropy. The local magnetic fields B_r are drawn at random from a uniform distribution in the interval $[-W, W]$. Thus, translation invariance and integrability of the model are broken for any $W \neq 0$. Total magnetization S^z is strictly conserved for any value of W . This model has been studied extensively in the context of MBL at $\Delta = 1$ and several exact-diagonalization studies find an MBL phase at infinite temperatures for $W/J \gtrsim 3.5$ [6, 9]. In this paper, we study the grand-canonical ensemble $\langle S^z \rangle = 0$, taking into account all S^z sectors.

The spin-current operator $j = J \sum_r (S_r^x S_{r+1}^y - S_r^y S_{r+1}^x)$ follows from the continuity equation. We are interested in the autocorrelation function at inverse temperatures $\beta = 1/T$ ($k_B = 1$), $C(t) = \text{Re} \langle j(t) j \rangle / L$, where the time argument of j has to be understood w.r.t. the Heisenberg picture, $j = j(0)$, and $C(0) = J^2/8$ at high temperatures $\beta \rightarrow 0$. From $C(t)$, we determine the optical conductivity via the Fourier transform

$$\text{Re } \sigma(\omega) = \frac{1 - e^{-\beta\omega}}{\omega} \int_0^{t_{\text{max}}} dt e^{i\omega t} C(t), \quad (2)$$

where the cut-off time t_{max} has to be chosen much larger than the relaxation time τ , with $C(\tau)/C(0) = 1/e$ [63, 64]. Note that, using the Jordan-Wigner transformation, H can be mapped onto interacting spinless fermions. In this picture, B_r is a disordered on-site chemical potential and j is the particle current.

Methods. We use the DQT method, which is most conveniently formulated in the time domain t and relies on the relation

$$C(t) = \text{Re} \frac{\langle \Phi_\beta(t) | j | \varphi_\beta(t) \rangle}{L \langle \Phi_\beta(0) | \Phi_\beta(0) \rangle} + \epsilon, \quad (3)$$

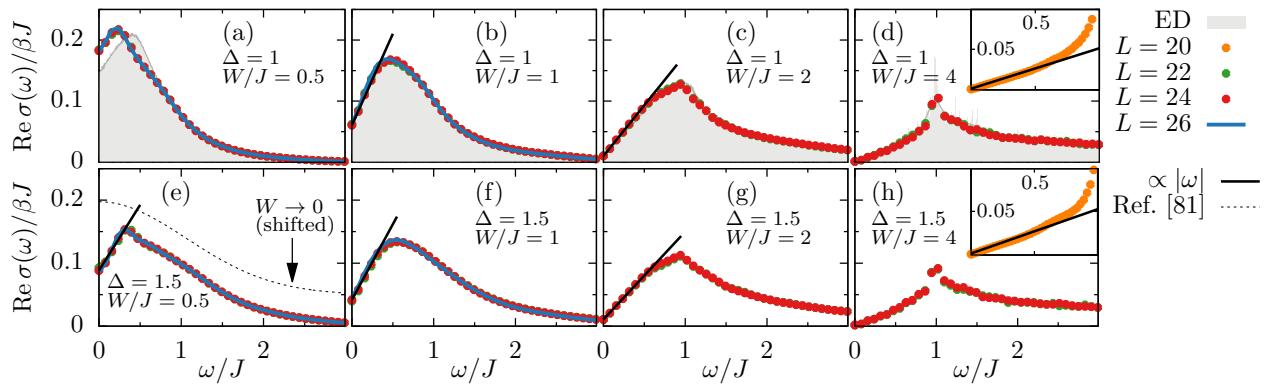


FIG. 3. (Color online) $\text{Re } \sigma(\omega)$ at $\beta \rightarrow 0$ for $\Delta = 1.0$ (upper row) and $\Delta = 1.5$ (lower row) in the transition from small $W/J = 0.5$ (l.h.s.) to strong $W/J = 4$ (r.h.s.) for the ensemble $\langle S^z \rangle = 0$, as obtained numerically for $L = 14$ using ED and $L > 14$ using DQT ($tJ \leq 40$; $L < 26$: $N = 200$, $L = 26$: $N = 20$). For $W = 4$, $L = 20$ data are shown for $N = 10000$ and $tJ \leq 120$ (insets), reducing statistical errors and increasing frequency resolution. In all cases (a)-(h), the low- ω behavior is well described by $\text{Re } \sigma(\omega) \approx \sigma_{\text{dc}} + a|\omega|$ (lines). In (e) the perturbative result of [47] for $W \rightarrow 0$ is depicted [87].

where $|\Phi_\beta(t)\rangle = e^{-iHt - \beta H/2} |\psi\rangle$, $|\varphi_\beta(t)\rangle = e^{-iHt} j e^{-\beta H/2} |\psi\rangle$, and $|\psi\rangle$ is a *single* pure state drawn at random. Most important, the remainder ϵ scales inversely with the partition function, i.e., ϵ is exponentially small in the number of thermally occupied eigenstates [43, 44, 68]. The great advantage of Eq. (3) is that it can be evaluated without any diagonalization by using forward-iterator algorithms. In this paper, we employ a fourth-order Runge-Kutta iterator with a discrete time step $\delta t J = 0.01 \ll 1$. Using this iterator, together with sparse-matrix representations of operators, we can reach system sizes as large as $L = 30$. However, since we have to average over $N \gg 1$ disorder realizations, we consider $L \leq 26$.

To additionally corroborate our DQT results, we employ ED for $L = 14$ and the finite-temperature Lanczos method (FTLM), formulated in the frequency domain ω and yielding $\text{Re } \sigma(\omega)$ with a frequency resolution $\delta\omega \propto 1/M$ [81], where $M \sim 400$ is the number of Lanczos steps used.

Results. We now present our DQT results, starting with the infinite-temperature limit $\beta \rightarrow 0$. As long not stated otherwise, all DQT data are obtained from real-time data $tJ \leq 40$, where the autocorrelation function $C(t)$ decays fully to zero [87]. This finite-time window yields a frequency resolution $\delta\omega/J \approx 0.08$.

First, for medium disorder $W/J = 2$, we compare in Fig. 2 the optical conductivity $\text{Re } \sigma(\omega)$, as obtained from DQT and FTLM for a system of size $L = 22$. The excellent agreement clearly shows that a single pure state, drawn at random from a high-dimensional Hilbert space, is a typical representative of the full statistical ensemble. This demonstration of typicality in disordered systems of finite size constitutes a first central result of our paper and is the fundament for using DQT as an accurate numerical method, for this and other values of W [87].

In Fig. 3 we summarize our optical-conductivity results $\text{Re } \sigma(\omega)$ for $\Delta = 1.0$ (upper row) and $\Delta = 1.5$ (lower row) along the transition from small disorder $W/J = 0.5$ (l.h.s.) to strong disorder $W/J = 4$ (r.h.s.). Several comments are in order. First, while finite-size effects increase as W decreases, we find no significant L dependence for large $L \geq 22$ in the disorder range $0.5 \leq W/J \leq 4.0$, depicted in Fig. 3. Second, while averaging over disorder realizations is more important for larger W , statistical errors for $N = 200$ are already smaller than the symbol size used for each W shown. Third, despite the large difference in L , the overall agreement with ED data, depicted for $L = 14$ in Fig. 3 (a)-(d), proves again that typicality is remarkably well satisfied. Finally, it is evident from Fig. 3 (a) that already at high T finite-size effects can be significant for $L = 14$.

As shown in Fig. 3, the optical conductivity $\text{Re } \sigma(\omega)$ has a well-defined value σ_{dc} at $\omega = 0$ and a maximum $\sigma_{\text{max}} > \sigma_{\text{dc}}$ located at $\omega_{\text{max}} > 0$ for all W depicted. While σ_{dc} decreases fast as W increases, σ_{max} has a much weaker W dependence, see Fig. 4 (b). In particular the position ω_{max} moves to higher frequencies and eventually saturates at large W , see Fig. 4 (c). Most notably, for $\omega \ll \omega_{\text{max}}$ the optical conductivity is well described by a power law, i.e., $\text{Re } \sigma(\omega) \approx \sigma_{\text{dc}} + a|\omega|^\alpha$, where $\alpha \approx 1$. The exponent $\alpha = 1$ has been proposed in [67] at the MBL transition. We find this exponent also in a wide range of the thermal phase. This finding does not depend on the frequency resolution and the disorder average, see Fig. 3 (d), (h), and can be substantiated by a log-log plot after subtracting σ_{dc} , see Fig. 4 (a). We further checked that our finding is true for binary disorder [87]. Note that the above power-law is different to Mott's law $\text{Re } \sigma(\omega) \propto \omega^\alpha$ with $\alpha = 2$, valid for $W/\Delta \gg 1$ [67]. Moreover, it differs from a subdiffusive power law with $\sigma_{\text{dc}} = 0$ and $\alpha < 1$ [82, 83], in agreement with Ref. [84].

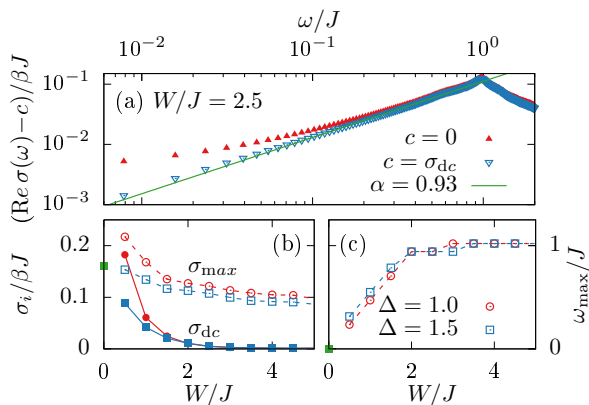


FIG. 4. (Color online) (a) Log-log plot of $\text{Re}\sigma(\omega) - c$, with $c = 0$ and $c = \sigma_{\text{dc}}$, at $W = 2.5$, $\Delta = 1$, and $\beta \rightarrow 0$ ($\langle S^z \rangle = 0$, $L = 20$, $tJ \leq 400$, $N = 1000$) as well as a power-law fit with the exponent $\alpha = 0.93$ being close to 1. (b), (c) Disorder dependence of σ_{dc} , the maximum σ_{max} , and its position ω_{max} at $\Delta = 1.0, 1.5$ and $\beta \rightarrow 0$ ($\langle S^z \rangle = 0$, $L = 24$, $tJ \leq 40$, $N = 200$). For $W = 0$, also the $\Delta = 1.5$ result of, e.g., [47] is indicated (green square).

For $W \rightarrow 0$, Fig. 4 (b), (c) suggests $\omega_{\text{max}} \rightarrow 0$ and $\sigma_{\text{dc}} = \sigma_{\text{max}}$ for $\Delta = 1.0$ and 1.5 . On the one hand, this suggestion is in line with results at $W = 0$ for $\Delta = 1.5$ in [47, 48, 85]. On the other hand, for $\Delta = 1.0$, the complete form of $\text{Re}\sigma(\omega)$ vs. ω is still under scrutiny [49–51, 57, 86], including the existence of a finite σ_{dc} .

Next, we turn to lower temperatures $\beta \neq 0$, focusing on $\Delta = 1$ and $W = 2$, where σ_{dc} is already small but still nonzero at $\beta = 0$. In Fig. 5 (a) we depict our results for $\text{Re}\sigma(\omega)\omega/(1 - e^{-\beta\omega})$, i.e., the mere Fourier transform of $C(t)$, for various $\beta J \leq 2$ and a single $L = 24$. Clearly, spectral weight at $\omega/J \gtrsim 2$ increases as β increases, while the overall structure at $\omega/J \sim 1$ only weakly depends on β . In Fig. 5 (b) we show the temperature dependence of σ_{dc} , which is well converged for $L \geq 20$ and $N \geq 500$ in the entire temperature range depicted. Apparently, at high temperatures, $\sigma_{\text{dc}}/\beta \approx \text{const}$. For $T/J \lesssim 2$, however, σ_{dc}/β decreases rapidly as T decreases. This finding is a central result of our paper. It is very suggestive of an interpretation in which extended states are frozen out below an energy scale of order $E - E_{\text{min}} \sim 2J$. Speaking differently, this result points to the existence of a *mobility edge* in terms of E , where E_{min} refers to the lower bound of the spectrum. Similar results have been reported in [65] for smaller values of W .

Summary and Conclusion. We studied the frequency dependence of the optical conductivity $\text{Re}\sigma(\omega)$ of the XXZ spin-1/2 chain in the transition from a thermal to a many-body localized phase induced by the strength of a spatially random magnetic field. To this end, we used numerical approaches to large system sizes, far beyond the applicability of standard ED, with a particular focus on DQT. In particular, we showed that the DQT

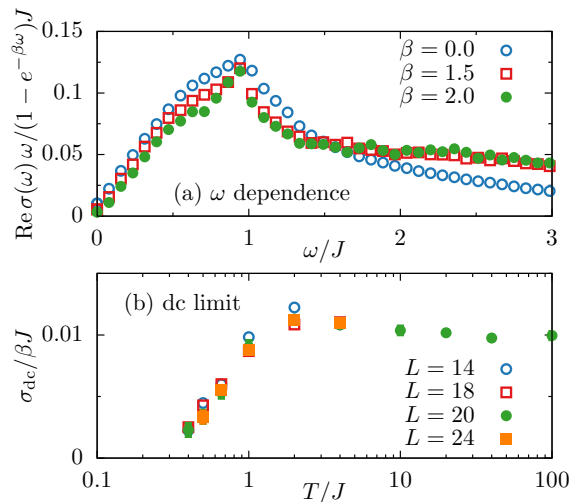


FIG. 5. (Color online) (a) $\text{Re}\sigma(\omega)$ at intermediate $W/J = 2$ and various $\beta J \leq 2$ for $\Delta = 1$ ($\langle S^z \rangle = 0$, $L = 24$, $tJ \leq 40$, $N = 1000$). (b) Temperature dependence of σ_{dc} for different $L \leq 24$. (Small error bars for the two largest $L = 20$ and 24 indicate the difference between $N = 500$ and 1000 .) This temperature dependence is consistent with a mobility edge located at $E - E_{\text{min}} \sim 2J$.

approach represents a powerful tool to study dynamical responses of MBL systems. First, we demonstrated the validity of typicality in disordered systems. Then, we found that the low-frequency behavior of $\text{Re}\sigma(\omega)$ is well described by $\text{Re}\sigma(\omega) \approx \sigma_{\text{dc}} + a|\omega|^\alpha$, with a constant $\alpha \approx 1$ in a wide range of the thermal phase and close to the transition. We further detailed the decrease of σ_{dc} as a function of increasing disorder or decreasing temperature. We particularly found that the temperature dependence is consistent with the existence of a mobility edge.

Acknowledgments. We thank X. Zotos, P. Prelovšek, and F. Heidrich-Meisner for fruitful discussions. J.H. acknowledges support by the EU program FP7-REGPOT-2012-2013-1 under Grant No. 316165. Work of W.B. and F.P. has been supported in part by the DFG through SFB 1143 and the NSF under Grant No. NSF PHY11-25915. W.B. also acknowledges kind hospitality of the PSM, Dresden. R.S. thanks the MPIPCKS, Dresden and the CCQCN, Crete for kind hospitality.

* rsteinig@uos.de

† jacek@physics.uoc.gr

‡ frankp@pks.mpg.de

§ w.brenig@tu-bs.de

- [1] P. W. Anderson, Phys. Rev. **109**, 1492 (1958).
- [2] D. M. Basko, I. L. Aleiner, and B. L. Altshuler, Ann. Phys. **321**, 1126 (2006).
- [3] J. M. Deutsch, Phys. Rev. A **43**, 2046 (1991).

- [4] M. Srednicki, Phys. Rev. E **50**, 888 (1994).
- [5] M. Rigol, V. Dunjko, and M. Olshanii, Nature **452**, 854 (2008).
- [6] A. Pal and D. A. Huse, Phys. Rev. B **82**, 174411 (2010).
- [7] V. Oganesyan and D. A. Huse, Phys. Rev. B **75**, 155111 (2007).
- [8] S. Bera, H. Schomerus, F. Heidrich-Meisner, and J. H. Bardarson, Phys. Rev. Lett. **115**, 046603 (2015).
- [9] D. J. Luitz, N. Laflorencie, and F. Alet, Phys. Rev. B **91**, 081103 (2015).
- [10] M. Žnidarič, T. Prosen, and P. Prelovšek, Phys. Rev. B **77**, 064426 (2008).
- [11] J. H. Bardarson, F. Pollmann, and J. E. Moore, Phys. Rev. Lett. **109**, 017202 (2012).
- [12] R. Vosk and E. Altman, Phys. Rev. Lett. **110**, 067204 (2013).
- [13] M. Serbyn, Z. Papic, and D. A. Abanin, Phys. Rev. Lett. **111**, 127201 (2013).
- [14] D. A. Huse, R. Nandkishore, and V. Oganesyan, Phys. Rev. B **90**, 174202 (2014).
- [15] D. A. Huse *et al.*, Phys. Rev. B **88**, 014206 (2013).
- [16] J. Kjäll, J. H. Bardarson, and F. Pollmann, Phys. Rev. Lett. **113**, 107204 (2014).
- [17] D. Pekker *et al.*, Phys. Rev. X **4**, 011052 (2014).
- [18] A. Chandran, V. Khemani, C. R. Laumann, and S. L. Sondhi, Phys. Rev. B **89**, 144201 (2014).
- [19] Y. Bahri, R. Vosk, E. Altman, and A. Vishwanath, Nat. Commun. **6**, 7341 (2015).
- [20] M. Schreiber *et al.*, Science **349**, 842 (2015).
- [21] M. Ovadia *et al.*, Sci. Rep. **5** 13503 (2015).
- [22] X. Zotos and P. Prelovšek, *Transport in one-dimensional quantum systems* (Kluwer Academic Publishers, 2004).
- [23] D. C. Johnston *et al.*, Phys. Rev. B **61**, 9558 (2000).
- [24] A. V. Sologubenko *et al.*, Phys. Rev. Lett. **84**, 2714 (2000).
- [25] C. Hess *et al.*, Phys. Rev. B **64**, 184305 (2001).
- [26] C. Hess *et al.*, Phys. Rev. Lett. **98**, 027201 (2007).
- [27] N. Hlubek *et al.*, Phys. Rev. B **81**, 20405R (2010).
- [28] K. R. Thurber *et al.*, Phys. Rev. Lett. **87**, 247202 (2001).
- [29] S. Trotzky *et al.*, Science **319**, 295 (2008).
- [30] P. Gambardella, Nature Mat. **5**, 431 (2006).
- [31] M. Kruczenski, Phys. Rev. Lett. **93**, 161602 (2004).
- [32] Y. B. Kim, Phys. Rev. B **53**, 16420 (1996).
- [33] B. S. Shastry and B. Sutherland, Phys. Rev. Lett. **65**, 243 (1990).
- [34] B. N. Narozhny, A. J. Millis, and N. Andrei, Phys. Rev. B **58**, 2921R (1998).
- [35] X. Zotos, Phys. Rev. Lett. **82**, 1764 (1999).
- [36] J. Benz *et al.*, J. Phys. Soc. Jpn. **74**, 181 (2005).
- [37] S. Fujimoto and N. Kawakami, Phys. Rev. Lett. **90**, 197202 (2003).
- [38] T. Prosen, Phys. Rev. Lett. **106**, 217206 (2011).
- [39] T. Prosen and E. Ilievski, Phys. Rev. Lett. **111**, 057203 (2013).
- [40] J. Herbrych, P. Prelovšek, and X. Zotos, Phys. Rev. B **84**, 155125 (2011).
- [41] C. Karrasch, J. H. Bardarson, and J. E. Moore, Phys. Rev. Lett. **108**, 227206 (2012).
- [42] C. Karrasch *et al.*, Phys. Rev. B **87**, 245128 (2013).
- [43] R. Steinigeweg, J. Gemmer, and W. Brenig, Phys. Rev. Lett. **112**, 120601 (2014).
- [44] R. Steinigeweg, J. Gemmer, and W. Brenig, Phys. Rev. B **91**, 104404 (2015).
- [45] J. M. P. Carmelo, T. Prosen, and D. K. Campbell, Phys. Rev. B **92**, 165133 (2015).
- [46] M. Žnidarič, Phys. Rev. Lett. **106**, 220601 (2011).
- [47] R. Steinigeweg and W. Brenig, Phys. Rev. Lett. **107**, 250602 (2011).
- [48] C. Karrasch, J. E. Moore, and F. Heidrich-Meisner, Phys. Rev. B **89**, 075139 (2014).
- [49] J. Sirker, R. G. Pereira, and I. Affleck, Phys. Rev. Lett. **103**, 216602 (2009).
- [50] J. Sirker, R. G. Pereira, and I. Affleck, Phys. Rev. B **83**, 035115 (2011).
- [51] S. Grossjohann and W. Brenig, Phys. Rev. B **81**, 012404 (2010).
- [52] E. Shimshoni, N. Andrei, and A. Rosch, Phys. Rev. B **72**, 059903 (2005).
- [53] A. V. Rozhkov and A. L. Chernyshev, Phys. Rev. Lett. **94**, 087201 (2005).
- [54] N. Hlubek *et al.*, J. Stat. Mech. **12**, P03006 (2012).
- [55] Y. Huang, C. Karrasch, J. E. Moore, Phys. Rev. B **88**, 115126 (2013).
- [56] C. Karrasch, R. Ilan, and J. E. Moore, Phys. Rev. B **88**, 195129 (2013).
- [57] F. Heidrich-Meisner *et al.*, Phys. Rev. B **68**, 134436 (2003).
- [58] R. Steinigeweg, J. Herbrych, P. Prelovšek, Phys. Rev. E **87**, 012118 (2013).
- [59] X. Zotos, Phys. Rev. Lett. **92**, 067202 (2004).
- [60] P. Jung, R. W. Helmes, and A. Rosch, Phys. Rev. Lett. **96**, 067202 (2006).
- [61] P. Jung and A. Rosch, Phys. Rev. B **76**, 245108 (2007).
- [62] C. Karrasch, D. M. Kennes, and F. Heidrich-Meisner, Phys. Rev. B **91**, 115130 (2015).
- [63] R. Steinigeweg *et al.*, Phys. Rev. B **90**, 094417 (2014).
- [64] R. Steinigeweg, J. Herbrych, X. Zotos, and W. Brenig, arXiv:1503.03871 (2015).
- [65] A. Karahalios *et al.*, Phys. Rev. B **79**, 024425 (2009).
- [66] O. S. Barišić and P. Prelovšek, Phys. Rev. B **82**, 161106 (2010).
- [67] S. Gopalakrishnan *et al.*, Phys. Rev. B **92**, 104202(2015).
- [68] T. A. Elsayed and B. V. Fine, Phys. Rev. Lett. **110**, 070404 (2013).
- [69] J. Gemmer and G. Mahler, Eur. Phys. J. B **31**, 249 (2003).
- [70] S. Goldstein *et al.*, Phys. Rev. Lett. **96**, 050403 (2006).
- [71] S. Popescu, A. J. Short, and A. Winter, Nature Phys. **2**, 754 (2006).
- [72] P. Reimann, Phys. Rev. Lett. **99**, 160404 (2007).
- [73] S. R. White, Phys. Rev. Lett. **102**, 190601 (2009).
- [74] C. Bartsch and J. Gemmer, Phys. Rev. Lett. **102**, 110403 (2009).
- [75] C. Bartsch and J. Gemmer, EPL **96**, 60008 (2011).
- [76] S. Sugiura and A. Shimizu, Phys. Rev. Lett. **108**, 240401 (2012).
- [77] S. Sugiura and A. Shimizu, Phys. Rev. Lett. **111**, 010401 (2013).
- [78] A. Hams and H. De Raedt, Phys. Rev. E **62**, 4365 (2000).
- [79] T. Iitaka and T. Ebisuzaki, Phys. Rev. Lett. **90**, 047203 (2003).
- [80] T. Iitaka and T. Ebisuzaki, Phys. Rev. E **69**, 047203 (2003).
- [81] A recent review is given in: P. Prelovšek and J. Bonča, *Ground State and Finite Temperature Lanczos Methods in Strongly Correlated Systems*, Solid-State Sciences 176 (Springer, Berlin, 2013).
- [82] K. Agarwal, S. Gopalakrishnan, M. Knap, M. Müller,

and E. Demler, Phys. Rev. Lett. **114**, 160401 (2015).

- [83] I. Khait, S. Gazit, N. Y. Yao, and A. Auerbach, arXiv:1603.06588 (2016).
 [84] O. S. Barišić, J. Kokalj, I. Balog, and P. Prelovšek, arXiv:1603.01526 (2016).
 [85] P. Prelovšek *et al.*, Phys. Rev. B **70**, 205129 (2004).
 [86] J. Herbrych, R. Steinigeweg, and P. Prelovšek, Phys. Rev. B **86**, 115106 (2012).
 [87] See Supplemental Material.

SUPPLEMENTAL MATERIAL

Time Dependencies

Intermediate Times

In our paper, we discussed the frequency dependence of the optical conductivity $\text{Re } \sigma(\omega)$ rather than the time dependence of the spin-current autocorrelation function $C(t)$ as such. However, we determined $\text{Re } \sigma(\omega)$ via the finite-time Fourier transform of $C(t)$. Furthermore, it is instructive to discuss the real-time decay of $C(t)$. Thus, we show in Fig. S1 the time-dependent data underlying Fig. 3 in our paper.

Clearly, for all $0.5 \leq W/J \leq 4.0$ and the two $\Delta = 1.0$ and 1.5 depicted, the initial value $C(0)$ agrees well with the sum rule $J^2/8$, which also shows the accuracy of our DQT approach. For all W depicted, the initial decay of $C(t)$ is fast with a relaxation time $\tau J \ll 10$. It is clearly visible that $C(t)$ develops oscillatory behavior for large W , which is the origin of the maximum σ_{max} located at the position ω_{max} , as discussed in our paper. However, all oscillations fully decay on a time scale $tJ \leq 40$ and there is no signature of a conserved Drude-weight contribution to $C(t)$ in the long-time limit. Therefore, $tJ \leq 40$ data is sufficient to precisely determine the ω dependence of $\text{Re } \sigma(\omega)$ in general and the value of σ_{dc} in particular.

Long Times

In Fig. S2 (a) we show $C(t)$ at $\Delta = 1$ and $W/J = 3.5$ for even longer times $tJ \leq 400$ and as many as $N = 30000$ disorder realizations in a system of size $L = 18$. Clearly, $C(t)$ is practically zero for $tJ \gtrsim 50$. Thus, while taking into account $tJ \leq 400$ in the Fourier transform certainly increases frequency resolution, we find no change of the linear frequency dependence down to a rather small scale of frequency, see Fig. S2 (b). It is worth mentioning that the $W/J = 3.5$ calculation depicted in Fig. S2 took about 20 CPU years in total.

In Fig. S2 we also depict high-resolution data for the same set of parameters except for $W/J = 2.0, 2.5$ and $N = 5000$, cf. Fig. 4 in the main text. Apparently, this data is well described by power laws with the exponent α being close to 1 in both cases.

Binary Disorder

Our paper focused on local magnetic fields B_r drawn at random from a uniform distribution in the interval $[-W, W]$. To demonstrate that the results presented do not depend on the specific distribution used, we repeat the $\Delta = 1.5$ calculations for $W/J = 1.0$ and $W/J = 2.0$ in Fig. 3 (f) and (g) for a binary distribution with the same width, i.e., $B_r = \pm\sqrt{3}W$. In Fig. S3 we compare the corresponding results. Evidently, the low- ω behavior of the optical conductivity $\text{Re } \sigma(\omega)$ is the same for both distributions, while differences can only be seen in the high- ω behavior, emerging for strong disorder W . These differences are not relevant for the physics discussed in our paper.

Finite-Size Effects: Comparison to Clean Systems

We found in our paper that the optical conductivity $\text{Re } \sigma(\omega)$ has a maximum $\sigma_{\text{max}} > \sigma_{\text{dc}}$ located at a position $\omega_{\text{max}} > 0$. Moreover, we observed little finite-size effects for large $L \geq 22$. Even though not expected, we cannot exclude a very slow convergence to the thermodynamic limit $L \rightarrow \infty$. Note that estimating potential finite-size effects on the basis of the non-interacting case $\Delta = 0$ is not meaningful for two reasons: First, for $\Delta = 0$ and $W > 0$, the localization length represents a natural scale for finite-size effects but is absent in the thermal phase of the $\Delta > 0$ problem. Second, also the case $\Delta = W = 0$ is well-known to feature huge finite-size effects because of the highly degenerated spectrum. Moreover, the mean free path is infinitely large.

Non-Integrable Systems

To provide further evidence for finite-size effects being negligibly small, we compare to results for cases without disorder, i.e., $W = 0$. For such cases, and $\Delta = 1.5$, the diffusion constant can be estimated perturbatively along the lines of [S1], yielding $D/J \sim 0.6$. This value of D corresponds to a mean free path of a few lattice sites, i.e., the mean free path is small compared to typical system sizes considered. Thus, finite-size effects are most likely related to the Hilbert-space dimension being finite and not to a physical length scale as such. Note that this line of reasoning is also meaningful for disordered but thermal cases.

We again break the integrability of the XXZ spin-1/2 chain but now by adding to Eq. (1), where $W = 0$, the next-to-nearest neighbor interaction

$$H' = J \Delta' \sum_{r=1}^L S_r^z S_{r+2}^z \quad (\text{S1})$$

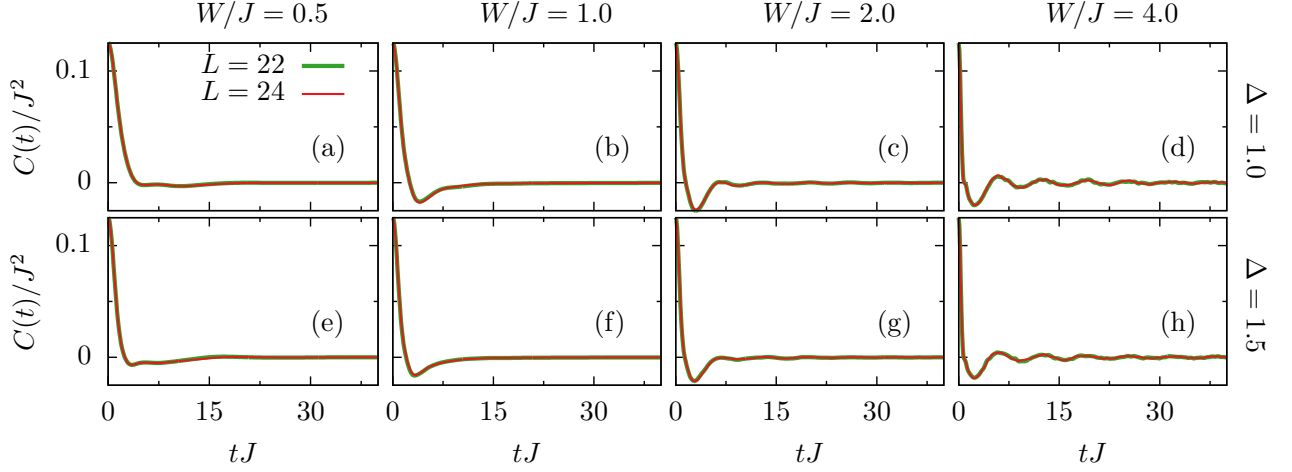


FIG. S1. (Color online) Data underlying Fig. 3 of the main text: Real-time decay of the high-temperature current autocorrelation function $C(t)$ of the spin-1/2 Heisenberg chain at (a)-(d) $\Delta = 1.0$ and (e)-(h) $\Delta = 1.5$ in the transition from (a), (e) small disorder $W/J = 0.5$ over intermediate disorder (b), (f) $W/J = 1.0$, (c), (g) $W/J = 2.0$ to strong disorder (d), (h) $W/J = 4.0$, as obtained numerically for the grand-canonical ensemble $\langle S^z \rangle = 0$ and system sizes $L = 22$ and 24 . The results shown are averaged over $N = 200$ different disorder realizations using a uniform distribution $[-W, W]$. The sum rule is $C(0)/J^2 = 0.125$. In all cases (a)-(h), $C(t)$ decays fully on a time scale $tJ \leq 40$. Damping of $C(t)$ after its first zero crossing causes the linear ω dependence $\text{Re} \sigma(\omega) \approx \sigma_{\text{dc}} + a|\omega|$.

with the anisotropy Δ' . Adding Eq. (S1) does not break translation invariance and does not change the form of the spin-current operator.

In Fig. S4 (a) we depict the high-temperature optical

conductivity $\text{Re} \sigma(\omega)$ for $\Delta = 1.5$ and $\Delta' = 0.5$, for a large $L = 30$ and a small enough $L = 22$ to illustrate the role of finite-size effects. It is clearly visible that, as long as $L \ll 30$, σ_{dc} decreases with L . Hence, together with the overall convergence at frequencies $\omega/J \gtrsim 0.4$, Fig. S4 (a) proves $\sigma_{\text{dc}} < \sigma_{\text{max}}$ in another model. Note that the

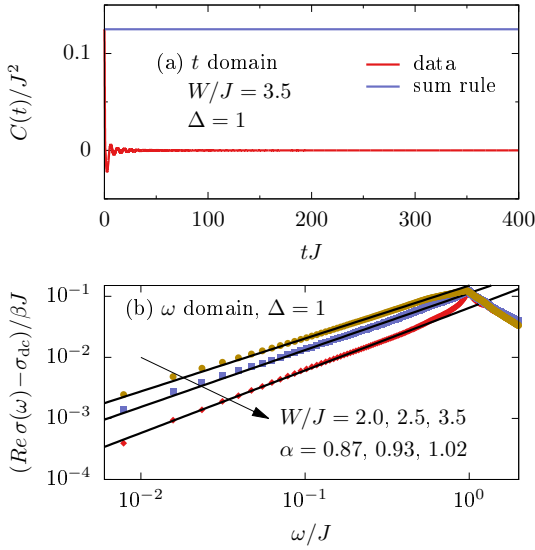


FIG. S2. (Color online) (a) Real-time decay of $C(t)$ for very long times $tJ \leq 400$, averaged over as many as $N = 30000$ disorder realizations in a system of size $L = 18$. Remaining parameters: $\Delta = 1$, $W/J = 3.5$, and $\beta J \rightarrow 0$. (b) Fourier transform of (a) and, additionally, for $W/J = 2.0, 2.5$ in a log-log plot. Remaining parameters: identical to (a) except for $N = 5000$. Note that σ_{dc} is subtracted from the Fourier transform. Power-law fits are also indicated.

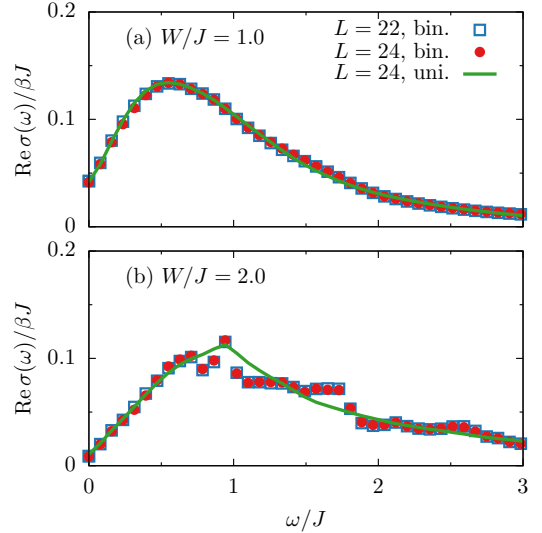


FIG. S3. (Color online) Optical conductivity $\text{Re} \sigma(\omega)$ for binary and uniform distribution and disorder strength (a) $W/J = 1$ and (b) $W/J = 2$. Remaining parameters: $\Delta = 1.5$, $\beta J \rightarrow 0$, $L \leq 24$, $tJ \leq 40$, and $N = 200$. Clearly, the low- ω behavior does not depend on the specific probability distribution used, while high- ω differences emerge for large W .

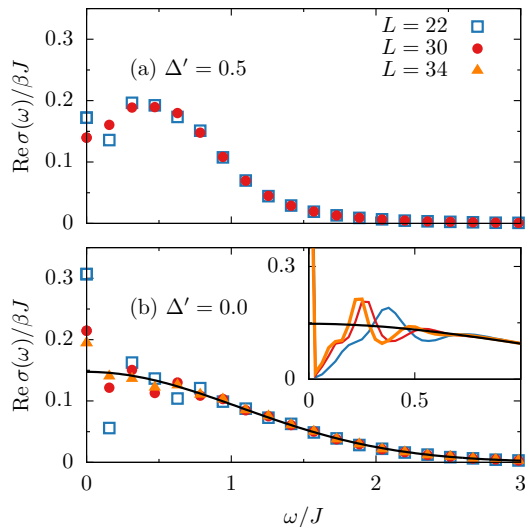


FIG. S4. (Color online) Optical conductivity $\text{Re} \sigma(\omega)$ for cases without disorder but with (a) $\Delta' = 0.5$ (non-integrable) and (b) $\Delta' = 0.0$ (integrable). Remaining parameters: $\Delta = 1.5$, $\beta J \rightarrow 0$, $L \leq 34$, $tJ \leq 20$, and $N = 1$. The solid line in (b) is the perturbative result of [S1]. Inset: (a) for $tJ \leq 100$, i.e., higher ω resolution.

largest-subspace dimension for $L = 30$ is comparable to the one of the $L = 26$ disordered model.

This ω dependence of $\text{Re} \sigma(\omega)$ has been found also in [S2] using Lanczos diagonalization and, for spin-1/2 ladders, in [S3] using time-dependent density-matrix renormalization group.

Integrable Systems

Eventually, we contrast all our results presented so far against the large finite-size effects in the integrable cases $W = \Delta' = 0$, as shown in Fig. S4 (b) for $\Delta = 1.5$. Here, $\text{Re} \sigma(\omega)$ is governed by finite-size effects at $\omega = 0$ and $\omega > 0$. Furthermore, these finite-size effects depend on the ω resolution used, see the inset of Fig. S4 (b). Thus, a very careful analysis is needed to determine correctly the thermodynamic limit [S1, S4, S5], yielding the dc value $\sigma_{\text{dc}}/\beta J \sim 0.15$. While this value is depicted in Fig. 4 (a) of our paper, none of our actual results rely on any kind of extrapolation.

Comparison to Exact and Lanczos Diagonalization

To additionally confirm the DQT results presented in our paper, we present results from two other numerical techniques: standard exact diagonalization (ED) and the finite-temperature Lanczos method (FTLM) [S7]. Both numerical techniques have direct access to the frequency domain. While ED data is binned in channels of width

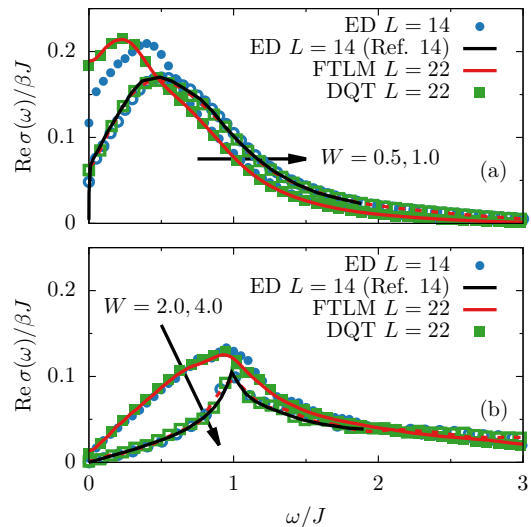


FIG. S5. (Color online) Optical conductivity $\text{Re} \sigma(\omega)$ at high temperatures $\beta \rightarrow 0$, as calculated by ED ($L = 14$), FTLM ($L = 22$), and DQT ($L = 22$), for the isotropic point $\Delta = 1.0$ and various disorder strengths (a) $W/J = 0.5, 1.0$ and (b) $W/J = 2.0, 4.0$. ED data for $W/J = 1.0, 4.0$ is taken from [S6].

$\delta\omega/J = 0.005$, the resolution of FTLM depends on the number of Lanczos steps M and the energy span ΔE , i.e., $\delta\omega \propto \Delta E/M$. Here, we use $M = 400$. Furthermore, we use 10 initial random vectors for each of the $N = 100$ disorder realizations, to decrease any remaining statistical error associated with the initial state.

In Fig. S5 we show ED ($L = 14$) and FTLM ($L = 22$) data for $\Delta = 1.0$, together with the DQT data ($L = 22$) presented in the main text. The overall agreement of all methods for $W \geq 1$ is remarkably good, despite the smaller system size $L = 14$ accessible to ED. For small W , significant finite-size effects are visible for $L = 14$. Note that ED data for $W/J = 1.0, 4.0$ is taken from [S6].

* rsteinig@uos.de

† jacek@physics.uoc.gr

‡ frankp@pks.mpg.de

§ w.brenig@tu-bs.de

[S1] R. Steinigeweg and W. Brenig, Phys. Rev. Lett. **107**, 250602 (2011).

[S2] M. Mierzejewski, J. Bonča, and P. Prelovšek, Phys. Rev. Lett. **107**, 126601 (2011).

[S3] C. Karrasch, D. M. Kennes, and F. Heidrich-Meisner, Phys. Rev. B **91**, 115130 (2015).

[S4] P. Prelovšek *et al.*, Phys. Rev. B **70**, 205129 (2004).

[S5] C. Karrasch, J. E. Moore, and F. Heidrich-Meisner, Phys. Rev. B **89**, 075139 (2014).

[S6] S. Gopalakrishnan *et al.*, Phys. Rev. B **92**, 104202(2015).

[S7] A recent review is given in: P. Prelovšek and J. Bonča, *Ground State and Finite Temperature Lanczos Methods*

in *Strongly Correlated Systems*, Solid-State Sciences 176
(Springer, Berlin, 2013).